

Spindle Speed Variation for the Suppression of Regenerative Chatter

N. Sri Namachchivaya and R. Beddini

Department of Aeronautical and Astronautical Engineering, University of Illinois at Urbana–Champaign, 306 Talbot Laboratory, 104 South Wright Street, Urbana, IL 61801, USA
e-mail: sri@nsgsun.aae.uiuc.edu

Received February 2, 2002; accepted January 6, 2003
Online publication April 16, 2003
Communicated by G. Stépán

Summary. A phenomenon commonly encountered during machining operations is chatter. It manifests itself as a vibration between workpiece and cutting tool, leading to poor dimensional accuracy and surface finish of the workpiece and to premature failure of the cutting tool. A chatter suppression method that has received attention in recent years is the spindle speed variation method, whereby greater widths of cut are achieved by modulating the spindle speed continuously. By adapting existing mathematical techniques, a perturbative method is developed in this paper to obtain finite-dimensional equations in order to systematically study the mechanism of spindle speed variation for chatter suppression. The results indicate both modest increase of stability and complex nonlinear dynamics close to the new stability boundary. The method developed in this paper can readily be applied to any other system with time-delay characteristics.

Key words. functional differential equation, multiple-time scale, chatter suppression, spindle speed variation

1991 Mathematics Subject Classification. 60F17

1. Introduction

Manufacturing technology relies heavily on material removal processes such as turning, milling, and drilling, where bulk material from a workpiece is removed by a tool which is much harder than the workpiece. Chatter, the self-excited relative vibration between workpiece and cutting tool, is a common problem in the machining process. Its adverse

Correspondence to: N. Sri Namachchivaya

effects include noise, poor surface finish, reduced dimensional accuracy, and shortened machine tool life. The onset of chatter acts as an upper bound on the width of cut for a specific cutting speed, limiting material-removal rates and productivity. The purpose of this paper is to clarify the mechanism of suppression of regenerative chatter through modulating the spindle speed continuously. We achieve this by analytical methods and evaluate the effects of the system parameters such as the amplitude and frequency of the spindle speed variation on the chatter suppression.

Various models have been developed to study chatter, all of which incorporate several mechanisms involved in different types of machining process. However, there is no widely accepted model in chatter studies. The models that take into consideration the so-called regenerative effect have gained more interest from researchers. Because of the existence of the regenerative effect, the forces acting on the cutting tools depend not only on the current states but on the past states as well. The equations governing the tool motion are differential equations with time-delay terms referred to as functional differential equations (FDE) [6], [27].

A recent book edited by Moon [20] explores both modeling and nonlinear dynamics phenomena in material-removal processes such as turning, milling, grinding, and rolling. While chatter in a turning operation is associated with the loss of fixed point stability of the corresponding FDE, the onset of chatter in a milling operation is related to the loss of stability of a periodic motion of the corresponding FDE. Furthermore, in a milling process, in addition to regenerative effect, it is important to consider loss of contact or impact dynamics as indicated by Balachandran [1].

Chatter can usually be avoided by maintaining a low material-removal rate, but clearly this is undesirable. Chatter suppression, a challenging problem in machining process research, is far from being solved. The need to suppress chatter has become stronger, especially in recent years, as the demands for high precision, high productivity, lower cost, and better working conditions are increasing. Intensive study has been done in this area, and various methods have been developed which may be used to overcome the problem of chatter without reducing material-removal rates. These methods involve passively modifying either the structure or the cutting tool and have included the use of vibration absorbers, variable pitch cutters, etc. In many cases, structural modifications may be expensive or technically difficult. A method of chatter suppression or elimination, applicable irrespective of machine cutter class and physical configuration, would clearly be beneficial.

One such method is the so-called Spindle Speed Variation (SSV), where the spindle speed is varied continuously to improve chatter performance. Takemura et al. [28] were the first to experimentally investigate the effect of spindle speed variation on tool vibration. Inamura and Sata [12], [13] provided, for the first time, a simple function space-based analysis of the stability of variable speed cutting. It was shown that a large increase in stability was attainable compared to cutting at constant speed. However, the limited experimental results indicated far more modest increases in stability. It was confirmed by Sexton et al. [24] that an invalid approximation in the theory [12], [13] resulted in predictions of large stability improvements. Sexton et al. [24], [25] used both experiments and analogue computer simulations to verify more modest increases in stability and thus explained some of the discrepancies in the previous theoretical work.

This method of continuous modulation of the spindle speed is attracting increasing attention because of its simplicity and effectiveness in chatter suppression (for details, see Lin et al. [18], Tsao et al. [29], Zhang et al. [30], and Jayaram et al. [15]). In this context, a numerical study based on Floquet theory for FDE was reported by Insperger et al. [14]. Typically the spindle speed is continuously varied through the superposition of a sinusoidally varying speed upon the original spindle speed, that is $\Omega(t) = \Omega_0 + \Delta\Omega \sin \nu t$, where Ω_0 is the mean spindle speed, $\Delta\Omega$, and ν are amplitude and frequency of the spindle speed variation. The determination of the amplitude $\Delta\Omega$ and the frequency ν for chatter suppression, at this stage, can be obtained only through experimentation or simulation. Thus the mechanism for this chatter suppression and the effects of nonlinearities on the periodically varying system are unclear.

The purpose of this paper is to study the delay differential equations with periodically perturbed delays using a functional analytic approach. Time delays are natural components of both biological [19] and physiological [10] systems, and there are numerous reasons for including them in the mathematical models to represent resource regeneration times, maturation periods, or reaction times, or to take into account the age structure in the population. Hence the unifying theme of *stabilization of delay differential equations with periodic delay* has broad applications beyond that of the machining or manufacturing processes. However, our focus in this paper is on the nonlinear dynamics and control of variable speed machining processes.

It would be of great significance if the mechanism of the SSV could be made clear through the development of a systematic analytic method, therefore obtaining the parameters crucial for SSV chatter control. The goal is to clarify the mechanism of suppression of regenerative chatter through modulating the spindle speed continuously and to determine stability boundaries and compute bifurcating solutions. Furthermore, experimental results and analogue computer simulations [24], [25] have confirmed that there were significant transient phenomena associated with variable speed cutting. Hence, a nonlinear investigation is essential to make sure that large amplitude transient tool vibrations do indeed decay with time. The main goal of this paper is to evaluate the effects of the system parameters such as the amplitude and frequency of the spindle speed variation on the chatter performance. To this end, we apply multiple-time scale sequential computations using the Fredholm alternative to determine stability boundaries and compute bifurcating solutions.

In a recent paper, Demir et al. [5] and Namachchivaya and Van Roessel [21] have examined the problem of suppression of regenerative chatter by augmenting the explicit time-dependent delay terms as new state variables to the original equations of motion with appropriate initial conditions. Both the Lyapunov-Schmidt [5] and center-manifold [21] methods were used to examine such augmented systems of delay differential equations with state dependent delay.

In Section 2, we present a widely accepted one degree of freedom model for the machine cutting process and incorporate the spindle speed variation in the mathematical model. In Section 3, we formulate the problem as perturbative functional differential equations and introduce the linear algebra on the space of continuous functions. We apply multiple-time scale sequential computations, using the Fredholm alternative, to determine two-dimensional reduced nonlinear equations, which represent the “normal form” of the original system with small periodic time delay. In Section 4, we examine the

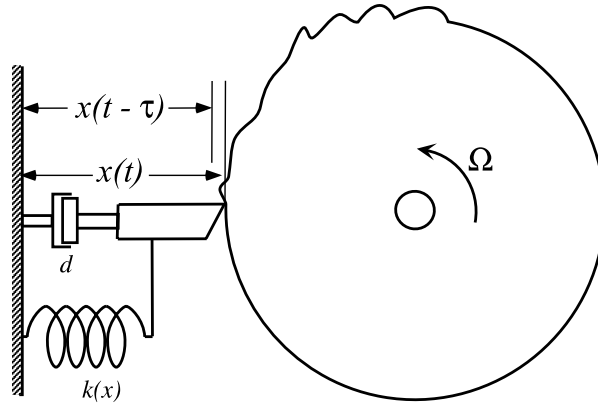


Fig. 1. Diagram of cutting wheel configuration and equivalent dynamical system.

stabilization or further destabilization of the trivial solution of the reduced equations and explain the mechanism of SSV in chatter suppression. We then present the bifurcating solutions of the reduced nonlinear system. In Section 5 the results and discussions of the analysis are presented with some recommendations for possible future work.

2. Hanna-Tobias Model and Spindle Speed Variation

Of the several mechanisms involved in chatter, the mechanism associated with the regenerative effect has gained the greatest attention from researchers. In regenerative chatter, the surface generated by the tool on one pass becomes the upper surface of the chip on the subsequent pass. Thus, the thickness of the chip and hence the forces acting on the cutting tool depend not only on its current state, but on its past state one revolution ago. Hence, nonlinear differential equations with time delay serve as convenient models. A widely accepted one degree of freedom model to describe regenerative cutting-tool chatter in turning or milling was developed by Hanna and Tobias [8]. A diagram of the cutting wheel configuration and effective spring-mass system is shown in Figure 2. Here, $k(x)$ is the “nonlinear” spring coefficient, and d is the effective damping. In this paper, we shall present a perturbative method to study the effects of spindle speed variation on the Hanna and Tobias model

$$\begin{aligned} \ddot{x}(t) + 2\zeta p\dot{x}(t) + p^2[x(t) + \beta_2 x^2(t) + \beta_3 x^3(t)] \\ = -\kappa p^2\{x(t) - x(t - \tau) + \hat{\beta}_2(x(t) - x(t - \tau))^2 + \hat{\beta}_3(x(t) - x(t - \tau))^3\}, \quad (1) \\ p^2 = \frac{k_0}{m}, \quad \zeta = \frac{\Delta p}{2\hat{\omega}}, \quad \Delta = \frac{h}{k_0}, \quad \kappa = \frac{k_1}{k_0} \end{aligned}$$

where $x(t)$ is the displacement normal to the machined surface at time t , m is the equivalent mass of the tool, k_0 is the linear stiffness, p is the natural frequency of the system, $h = \hat{\omega}d$ is the hysteretic damping coefficient, $\hat{\omega}$ is the chatter frequency which depends on system parameters, k_1 is the width-of-cut parameter. The regenerative effect

enters the equation of motion through chip thickness

$$s \stackrel{\text{def}}{=} x(t) - x(t - \tau), \quad \tau = \frac{1}{N} \quad \text{and} \quad N = z\Omega,$$

where Ω is the spindle speed, z is the number of cutter blades. Coefficients β_2 and β_3 are two constants describing the nonlinear stiffness of the machine tool such that the stiffness function is described by $k_0[x(t) + \beta_2x^2(t) + \beta_3x^3(t)]$, and $\hat{\beta}_2$ and $\hat{\beta}_3$ are constant coefficients of the nonlinear cutting force function which depends on chip thickness. These parameters are often evaluated empirically, and representative values are given in Appendix A. Details can be found in [8].

In order to obtain stability properties, we must first study the linear part of the *Hanna-Tobias* model (1),

$$\ddot{x}(t) + 2\zeta p\dot{x}(t) + p^2x(t) = -\kappa p^2\{x(t) - x(t - \tau)\}. \quad (2)$$

The corresponding characteristic equation is

$$\rho^2 + 2\zeta p\rho + p^2 = -\kappa p^2(1 - e^{-\rho\tau}). \quad (3)$$

For $\tau = 0$, equation (3) has two roots with negative real parts. As soon as $\tau > 0$, equation (3) is a transcendental equation and has infinitely many solutions for $\rho(\kappa, \tau) = \hat{\delta}(\kappa, \tau) + i\hat{\omega}(\kappa, \tau)$; hence it is an *infinite-dimensional problem*. These new roots may cross the imaginary axis as τ or κ is further increased. Thus, the first task is to determine these crossings which give rise to instability. Assuming that at $\kappa = \kappa_c$ and $\tau = \tau_c$ we have such a crossing, i.e.,

$$\rho = i\hat{\omega}_c, \quad \text{where} \quad \hat{\omega}_c \stackrel{\text{def}}{=} \hat{\omega}(\kappa_c, \tau_c),$$

is the critical chatter frequency, equation (3) yields

$$-\hat{\omega}_c^2 + p^2 = -\kappa_c p^2(1 - \cos \hat{\omega}_c \tau_c), \quad \Delta = -\kappa_c \sin \hat{\omega}_c \tau_c.$$

From the above equation, we find the critical value of the width-of-cut as

$$\kappa_c = \frac{\hat{\omega}_c^2 - p^2}{2p^2} + \frac{\Delta^2 p^2}{2(\hat{\omega}_c^2 - p^2)}. \quad (4)$$

Since the width-of-cut is positive, $\kappa_c > 0$, it is obvious from (4) that $\hat{\omega}_c > p$. It clearly states that the chatter frequency, $\hat{\omega}_c$, is always greater than the natural frequency, p , of the system. In addition, we have

$$\tau_c = \frac{2(\arctan(\frac{p^2 - \hat{\omega}_c^2}{\Delta p^2}) + k\pi)}{\hat{\omega}_c}, \quad k = 1, 2, 3, \dots, \quad (5)$$

and the *width-of-cut* κ and *time delay* τ are the natural control parameters in the machine cutting process. Equations (4) and (5), which are solved parametrically in terms of critical chatter frequency, $\hat{\omega}_c$, yield the conventional stability chart [8], given in Figure 2. The region within the parabolic lines (representing stability limits) is unstable. Furthermore,

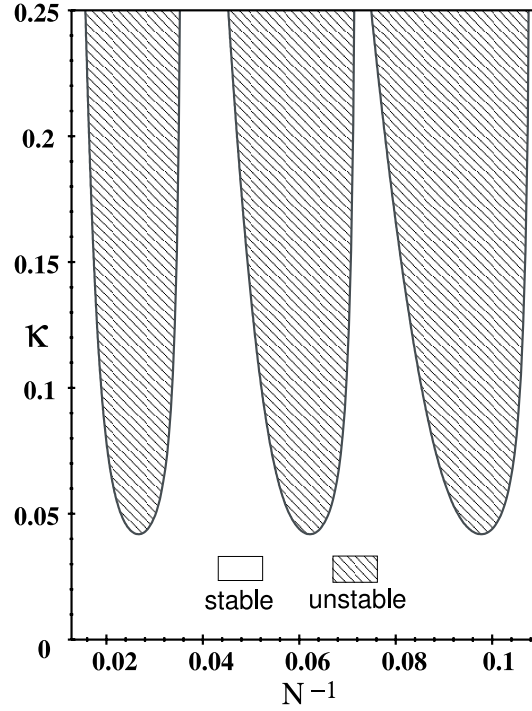


Fig. 2. Stability chart for $p = 173.25$, $\Delta = 0.041845$.

there is a lower bound of the stability limit which can easily be calculated from (4) as the minimum of the critical width-of-cut. The critical chatter frequency can also be explicitly calculated from the width-of-cut κ_c as

$$\hat{\omega}_c^2 = p^2(1 + \kappa_c) \pm p^2 \sqrt{\kappa_c^2 - (\Delta)^2}.$$

2.1. Spindle Speed Variation

As mentioned in the introduction, it has been shown by previous research [12], [13], [24] that greater widths of cut could be achieved without chatter by modulating the spindle speed continuously. To this end, we let

$$\tau \rightarrow \tau_0 + \epsilon \hat{\sigma}(t), \quad \text{where} \quad \hat{\sigma}(t) \stackrel{\text{def}}{=} \sum_{\substack{n \neq 0 \\ -1}}^1 \hat{\mu}_n e^{in\hat{\nu}t}, \quad (6)$$

as in Inamura and Sata [13], where $\hat{\mu}_{-n} = \bar{\hat{\mu}}_n$ and $\epsilon \ll 1$. The mean value of the period of spindle rotation, τ_0 , and complex constant, $\hat{\mu}_n$, are related to mean cutting speed, N , and the amplitude of spindle speed variation, $\pm \delta N$, as follows:

$$\tau_0 = \frac{N}{N^2 - (\delta N)^2}, \quad 2|\hat{\mu}_n| = \frac{\delta N}{N^2 - (\delta N)^2}, \quad \arg(\hat{\mu}_n) = \arccos\left(\frac{\delta N}{N}\right).$$

It has been found in experiments conducted by Inamura and Sata [13], Hosi and Sato [11], and Sexton et al. [24] that when the amplitude $\hat{\mu}_n$ and the frequency $\hat{\nu}$ are within some range, the chatter can be greatly suppressed or eliminated. Furthermore, it was shown that the natural frequency p of the machine tool is much higher than the frequency of spindle speed variation. Hence we shall assume that

$$\hat{\nu} < p < \hat{\omega}_c.$$

Rescaling time $t \rightarrow \frac{t}{\hat{\omega}_c}$ with $r_0 = \hat{\omega}_c \tau_0$ and defining the new variables

$$u(t) \stackrel{\text{def}}{=} x\left(\frac{\tau_0}{r_0}t\right), \quad u(t - r_0 - \varepsilon\sigma(t)) = x\left(\frac{\tau_0}{r_0}(t - r_0 - \varepsilon\sigma(t))\right),$$

$$\sigma(t) \stackrel{\text{def}}{=} \frac{r_0}{\tau_0}\hat{\sigma}\left(\frac{\tau_0}{r_0}t\right),$$

yield

$$\begin{aligned} \ddot{u}(t) + 2\zeta\omega_p\dot{u}(t) + \omega_p^2(1 + \kappa)u(t) - \kappa\omega_p^2u(t - r_0 - \varepsilon\sigma(t)) \\ = -\omega_p^2[\beta_2u^2(t) + \kappa\hat{\beta}_2(u(t) - u(t - r_0 - \varepsilon\sigma(t)))^2] \\ -\omega_p^2[\beta_3u^3(t) + \kappa\hat{\beta}_3(u(t) - u(t - r_0 - \varepsilon\sigma(t)))^3], \end{aligned} \quad (7)$$

where the normalized chatter, natural, and forcing frequencies are given as

$$\omega(\kappa, r_0) = \frac{\hat{\omega}(\kappa, \tau_0)}{\hat{\omega}_c}, \quad \omega_p = \frac{p}{\hat{\omega}_c}, \quad \nu = \frac{\hat{\nu}}{\hat{\omega}_c}.$$

The damping parameter, ζ , by definition is a function of the chatter frequency, and hence a function of the control parameters, κ and τ_0 . This fact, as we shall show later, makes the calculation of the transversality (or, crossing condition) (see Appendix A) more difficult. Since we are mainly interested in the effects of nonlinearities and spindle speed variations close to instability, we shall henceforth take the bifurcation parameter to be α , which can be either $(r_0 - r_c)$ or $(\kappa - \kappa_c)$. Furthermore, we shall denote the normalized eigenvalue of the linearized equations corresponding to (7) as $\lambda(\kappa, r_0) = \delta(\kappa, r_0) + i\omega(\kappa, r_0)$.

The purpose of this paper is to examine the effects of this periodic variation in delay ($\varepsilon \neq 0$) on the asymptotic stability of the trivial solution of (2) and the associated bifurcations close to the critical parameter, $\alpha = 0$. We hope that stabilization or further destabilization of the trivial solution for $\alpha > 0$ may explain the mechanism of SSV in chatter suppression.

3. Perturbative Analysis of Functional Differential Equations

Letting $x_1(t) = u(t)$, $x_2(t) = \dot{u}(t)$, and after simplification, we can write the original equation (7) into a set of first-order form as

$$\begin{aligned} \dot{X}(t) = \begin{pmatrix} 0 & 1 \\ -B(\alpha) & -A(\alpha) \end{pmatrix} X(t) + \begin{pmatrix} 0 & 0 \\ -C(\alpha) & 0 \end{pmatrix} X(t - r_0 - \varepsilon\sigma(t)) \\ + \begin{pmatrix} 0 \\ f(X(t), X(t - r_0 - \varepsilon\sigma(t)), \alpha) \end{pmatrix}, \end{aligned} \quad (8)$$

where

$$\begin{aligned} f(X(t), X(t - r_0 - \epsilon\sigma(t)), \alpha) = & c_{20}(\alpha)x_1^2(t) + c_{11}(\alpha)x_1(t)x_1(t - r_0 - \epsilon\sigma(t)) \\ & + c_{02}(\alpha)x_1^2(t - r_0 - \epsilon\sigma(t)) + c_{30}(\alpha)x_1^3(t) + c_{21}(\alpha)x_1^2(t)x_1(t - r_0 - \epsilon\sigma(t)) \\ & + c_{12}(\alpha)x_1(t)x_1^2(t - r_0 - \epsilon\sigma(t)) + c_{03}(\alpha)x_1^3(t - r_0 - \epsilon\sigma(t)), \end{aligned}$$

and the linear and nonlinear coefficients are given in Appendix A.

For the unperturbed ($\epsilon = 0$) system (corresponding to (8)), the characteristic equation at $\alpha = \alpha_c = 0$ has a pair of pure imaginary roots, which we normalize to one, $\lambda = \pm i$. This normalization of chatter frequency gives the following relations between the mean delay and the linear critical coefficients:

$$C_0 \cos r_0 = 1 - B_0, \quad C_0 \sin r_0 = A_0, \quad (9)$$

where $A_0 \stackrel{\text{def}}{=} A(0)$, $B_0 \stackrel{\text{def}}{=} B(0)$, $C_0 \stackrel{\text{def}}{=} C(0)$. We shall use the relations (9) to simplify some of the expressions in the subsequent sections. All the other roots of the characteristic equation, at $\alpha = \alpha_c = 0$, have negative real parts.

Both the center-manifold [3], [4], and the Lyapunov-Schmidt [9] reduction have been applied to determine the finite-dimensional bifurcation equations for the autonomous regenerative system (7) [17]. Though they can be used with some modifications to construct solutions in the periodically modulated delay equations (8) as shown in [5], [21], they in fact involve some redundant computations. Instead, we apply the multiple-time scale method with sequential computations using the Fredholm alternative to determine the stability boundary and to compute bifurcating solutions.

The growth or decay of the solutions of (8), close to the critical bifurcation parameter, due to periodic variation is expected to occur in a much slower time scale $s \stackrel{\text{def}}{=} \epsilon^2 t$. This was also pointed out by Nayfeh et al. [22] in the context of Hopf bifurcations in constant speed chatter dynamics. Hence, we introduce a third-order multiple-time solution of the form

$$X(t) = X(t, s; \epsilon) \stackrel{\text{def}}{=} \sum_{i=1}^3 \epsilon^i X^i(t, s) + h.o.t. \quad (10)$$

Then we can evaluate

$$\dot{X}(t) = \dot{X}(t, s; \epsilon) = \sum_{i=1}^3 \left(\epsilon^i \frac{\partial X^i}{\partial t} + \epsilon^{i+2} \frac{\partial X^i}{\partial s} \right) + h.o.t., \quad (11)$$

and expand $X^i(t - r_0 - \epsilon\sigma(t), s - \epsilon^2(r_0 + \epsilon\sigma(t)))$ as a Taylor series in ϵ

$$\begin{aligned} X^i(t - r_0 - \epsilon\sigma(t), s - \epsilon^2(r_0 + \epsilon\sigma(t))) = & X^i(t - r_0, s) - \epsilon\sigma(t) \frac{\partial X^i}{\partial t}(t - r_0, s) \\ & + \epsilon^2 \left(\frac{\sigma^2(t)}{2} \frac{\partial^2 X^i}{\partial t^2}(t - r_0, s) - r_0 \frac{\partial X^i}{\partial s}(t - r_0, s) \right) + h.o.t. \end{aligned}$$

Substituting these expressions, taking $\alpha \rightarrow \epsilon^2 \alpha$ in (8), and equating coefficients of the first three orders of ϵ , we obtain

$$\mathcal{L}(X^1)(t, s) = 0, \quad \mathcal{L}(X^2)(t, s) = \mathcal{F}^2(t, s), \quad \mathcal{L}(X^3)(t, s) = \mathcal{F}^3(t, s), \quad (12)$$

where we define

$$\mathcal{L}(X^i)(t, s) \stackrel{\text{def}}{=} -\frac{\partial X^i}{\partial t}(t, s) + \begin{pmatrix} 0 & 1 \\ -B_0 & -A_0 \end{pmatrix} X^i(t, s) + \begin{pmatrix} 0 & 0 \\ -C_0 & 0 \end{pmatrix} X^i(t - r_0, s),$$

and the inhomogeneous terms are given explicitly as

$$\begin{aligned} \mathcal{F}^2(t, s) &= C_0 \begin{pmatrix} 0 \\ -\sigma(t)x_2^1(t - r_0, s) \end{pmatrix} \\ &\quad + \begin{pmatrix} 0 \\ -c_{20}(x_1^1)^2(t, s) - c_{11}x_1^1(t, s)x_1^1(t - r_0, s) - c_{02}(x_1^1)^2(t - r_0, s) \end{pmatrix} \\ \mathcal{F}^3(t, s) &= C_0 \begin{pmatrix} 0 \\ -\sigma(t)x_2^2(t - r_0, s) + \frac{\sigma^2(t)}{2}\frac{\partial x_2^1}{\partial t}(t - r_0, s) - r_0\frac{\partial x_1^1}{\partial s}(t - r_0, s) \end{pmatrix} \\ &\quad + \alpha \begin{pmatrix} 0 \\ A_1x_2^1(t, s) + B_1x_1^1(t, s) + C_1x_1^1(t - r_0, s) \end{pmatrix} + \begin{pmatrix} \frac{\partial x_1^1(t, s)}{\partial s} \\ \frac{\partial x_2^1(t, s)}{\partial s} \end{pmatrix} \\ &\quad + \sigma(t) \begin{pmatrix} 0 \\ +c_{11}x_1^1(t, s) + 2c_{02}x_1^1(t - r_0, s) \end{pmatrix} x_2^1(t - r_0, s) \\ &\quad - 2 \begin{pmatrix} 0 \\ c_{20}x_1^1(t, s)x_1^2(t, s) + c_{02}x_1^2(t - r_0, s)x_1^1(t - r_0, s) \end{pmatrix} \\ &\quad - c_{11} \begin{pmatrix} 0 \\ x_1^2(t, s)x_1^1(t - r_0, s) + x_1^1(t, s)x_1^2(t - r_0, s) \end{pmatrix} \\ &\quad - \begin{pmatrix} 0 \\ c_{30}(x_1^1)^3(t, s) + c_{03}(x_1^1)^3(t - r_0, s) \end{pmatrix} \\ &\quad - \begin{pmatrix} 0 \\ c_{21}(x_1^1)^2(t, s)x_1^1(t - r_0, s) + c_{12}x_1^1(t, s)(x_1^1)^2(t - r_0, s) \end{pmatrix}. \end{aligned}$$

It is worth pointing out that, although the highest derivative term in the expression for $\mathcal{F}^3(t, s)$ contains delay, we shall treat the resulting perturbation equations as DDE (as opposed to Neutral DE) due to the fact it enters at $\mathcal{O}(\varepsilon^2)$. Further, the scaling of the unfolding parameter α to $\mathcal{O}(\varepsilon^2)$ is natural since the system has both quadratic and cubic nonlinearities and exhibits a Hopf bifurcation. It is the correct scaling because the unfolding parameter has to be at the same order as the leading order nonlinear term in the normal form, which in our case will clearly be $\mathcal{O}(\varepsilon^2)$.

Equation (12) represents an inhomogeneous FDE of the form

$$\mathcal{L}(X^i)(t, s) = \mathcal{F}^i(t, s), \tag{13}$$

with a solution space of infinite dimension. The theory of the FDE [2], [4], [6], [7] has been developed well enough to a point of high sophistication and provides amazingly

successful descriptions of the nonlinear cutting tool dynamics. Suppose $r_0 \geq 0$ is a given real number, \mathbb{R}^2 is a two-dimensional linear vector space over the reals with norm $|\cdot|$, $\mathcal{C}([-r_0, 0], \mathbb{R}^2)$ is the Banach space of continuous functions mapping the interval $[-r_0, 0]$ into \mathbb{R}^2 with the topology of uniform convergence, and designate the norm of an element ϕ in \mathcal{C} by $|\phi| = \sup_{-r_0 \leq \theta \leq 0} |\phi(\theta)|$. If

$$\sigma \in \mathbb{R}, \quad a \geq 0, \quad X \in \mathcal{C}([-\sigma - r_0, \sigma + a], \mathbb{R}^2),$$

then for any $t \in [\sigma, \sigma + a]$, we let $X_t \in \mathcal{C}$ be defined by $X_t(\theta; s) = X(t + \theta; s)$, $-r_0 \leq \theta \leq 0$. Introducing the “new variable” $X_t^i(\theta; s) = X^i(t + \theta; s)$, we have

$$\dot{X}_t^i(\theta; s) = \begin{cases} \frac{dX_t^i(\theta^+; s)}{d\theta}, & -r_0 \leq \theta < 0, \\ LX_t^i - \mathcal{F}^i(t, s), & \theta = 0, \end{cases} \quad i = 1, \dots, 3, \quad (14)$$

where

$$LX_t^i(\theta) = \int_{-r_0}^0 [d\eta(\theta)] X^i(t + \theta; s) \quad (15)$$

and

$$[d\eta(\theta)] = \begin{pmatrix} 0 & 1 \\ -B_0 & -A_0 \end{pmatrix} \delta(\theta) + \begin{pmatrix} 0 & 0 \\ -C_0 & 0 \end{pmatrix} \delta(\theta + r_0). \quad (16)$$

It is very important to realize that (14) is the *starting point* for the rest of our analysis. Some facts about the homogeneous equation are given in Appendix B.

At $\theta = 0$, equation (14) is just equation (13)

$$\dot{X}^i(t, s) = \int_{-r_0}^0 [d\eta(\theta)] X^i(t + \theta; s) - \mathcal{F}^i(t, s), \quad i = 1, \dots, 3, \quad (17)$$

which is to be solved at each stage of the perturbations. Hence, before proceeding with the determination of solutions, let us state an important result (Lemma 3.1).

We seek a 2π -periodic solution of (17), where $\mathcal{F}^i(t, s)$ 2π -periodic. To this end, suppressing the slow-time parameter s , define the operator J acting on a Banach space

$$C_{2\pi} \stackrel{\text{def}}{=} \{f: f(s+2\pi) = f(s), f \in \mathcal{C}([0, 2\pi], \mathbb{R}^2)\}, \quad \text{with norm } \|f\| = \sup_{0 \leq s \leq 2\pi} |f(s)|,$$

as

$$JX^i(t) \stackrel{\text{def}}{=} -\frac{d}{dt} X^i(t) + LX_t^i, \quad (18)$$

where the domain of $\mathcal{D}(J)$ is $C_{2\pi}^1$ with the standard norm. From the definition, it is easy to show that the null space of J is

$$\mathcal{N}(J) = \left(\eta \stackrel{\text{def}}{=} \xi(0)e^{is}, \bar{\eta} \stackrel{\text{def}}{=} \bar{\xi}(0)e^{-is} \right),$$

where $\xi(0)$ satisfies (39). Also the formal adjoint operator, J^* , of J is defined as

$$J^* X^i(t) \stackrel{\text{def}}{=} \frac{d}{ds} X^i(t) + L^* X_t^i, \quad (19)$$

and the null space of J^* ,

$$\mathcal{N}(J^*) = \left(\eta^* \stackrel{\text{def}}{=} \xi^*(0)e^{is}, \bar{\eta}^* \stackrel{\text{def}}{=} \bar{\xi}^*(0)e^{-is} \right),$$

where $\xi^*(0)$ satisfies (40). The linear operator, J , has the *Fredholm alternative* property in the space $C_{2\pi}$ (see [6], Chapter 9) where the inner product is defined by

$$\ll v(t), u(t) \gg \stackrel{\text{def}}{=} \frac{1}{2\pi} \int_0^{2\pi} (v(t), u(t)) dt. \tag{20}$$

This implies that $\mathcal{R}(J) = \mathcal{N}^\perp(J^*)$ and $\mathcal{N}(J) = \mathcal{N}(J^*)$. It is also easy to check that $\mathcal{N}(J) \cap \mathcal{R}(J) = \{0\}$.

Rewriting the inhomogeneous equations (17) as

$$JX^i(t) = \mathcal{F}^i(t), \quad \mathcal{F}^i \in C_{2\pi}, \quad i = 2, 3, \tag{21}$$

we have

Lemma 3.1. *Equation (21) is solvable for $X^i(t; s) \in \mathcal{D}(J)$ if and only if*

$$\ll \mathcal{F}^i, \eta^* \gg = \ll \mathcal{F}^i, \bar{\eta}^* \gg = 0. \tag{22}$$

Furthermore, there is a continuous projection, $\mathbf{P}: C_{2\pi} \rightarrow C_{2\pi}$, such that the range of J is obtained by subtracting off part of $f \in C_{2\pi}$, namely $\mathbf{P}f$, so that the orthogonality conditions (22) are satisfied, that is,

$$\mathcal{R}(J) = (\mathbf{I} - \mathbf{P})C_{2\pi},$$

and there is a continuous linear operator

$$\mathbf{K}: (\mathbf{I} - \mathbf{P})C_{2\pi} \rightarrow (\mathbf{I} - \mathbf{P})C_{2\pi} \cap \mathcal{D}(J),$$

such that $\mathbf{K}\mathcal{F}^i$ is a solution of (21) for each $\mathcal{F}^i \in (\mathbf{I} - \mathbf{P})C_{2\pi}$, where \mathbf{P} is a continuous projection of $C_{2\pi}$ onto $\mathcal{N}(J)$.

Proof. Straightforward application of Hale's ([6]; Chapter 7) results on necessary and sufficient conditions for the existence of periodic solutions of nonhomogeneous linear functional equations. \square

The Fredholm alternative and the solvability condition (22) will be used in the sequential computations to determine and compute bifurcating solutions.

3.1. The Solution to $\mathcal{O}(1)$

From the discussions in Appendix B, it is clear that the solution of

$$\dot{X}_t^1(\theta; s) = \mathbf{A}X_t^1(\theta; s) \tag{23}$$

is given by

$$X_t^1(\theta; s) = z(s)\xi(\theta) \exp\{it\} + \text{c.c.}, \quad \text{where } \xi(\theta) = \begin{pmatrix} 1 \\ i \end{pmatrix} e^{i\theta}, \quad (24)$$

where c.c. is the abbreviation for complex conjugate and $z(s)$ is an unknown function of the slow-time s .

3.2. The Solution to $\mathcal{O}(\varepsilon)$

Inserting the expression for $X_t^1(\theta; s)$ from (24) into (14) and using the definition of $\sigma(t)$ from (6) yields

$$\dot{X}_t^2(\theta; s) = \begin{cases} \frac{dX_t^2(\theta^+; s)}{d\theta}, & -r_0 \leq \theta < 0, \\ LX_t^2(\theta; s) - \mathcal{F}^2(t; s), & \theta = 0, \end{cases}$$

where

$$\begin{aligned} \mathcal{F}^2(t; s) = & -iz(s) \sum_{\substack{n \neq 0 \\ -1}}^1 \begin{pmatrix} 0 \\ C_0 \xi_1(-r_0) \mu_n \end{pmatrix} e^{i(1+n\nu)t} + \text{c.c.} \\ & - z^2(s) \begin{pmatrix} 0 \\ c_{11} \xi_1(0) \xi_1(-r_0) + c_{02} \xi_1^2(-r_0) + c_{20} \xi_1^2(0) \end{pmatrix} e^{2it} + \text{c.c.} - |z(s)|^2 \\ & \times \begin{pmatrix} 0 \\ c_{11}(\xi_1(0) \bar{\xi}_1(-r_0) + \bar{\xi}_1(0) \xi_1(-r_0)) + 2c_{20} |\xi_1|^2(0) + 2c_{02} |\xi_1|^2(-r_0) \end{pmatrix} \end{aligned}$$

Making use of the fact that the frequency of the spindle speed modulation, ν , is much smaller than the chatter frequency, the nonhomogeneous equation at $\theta = 0$,

$$JX^2(t; s) = \mathcal{F}^2(t; s), \quad (25)$$

is solvable for $X^2(t; s) \in \mathcal{D}(J)$. The solution is given explicitly as

$$\begin{aligned} X_t^2(\theta; s) = & z(s) C_0 \xi_1(-r_0) \sum_{\substack{n \neq 0 \\ -1}}^1 \frac{\mu_n}{\mathcal{N}_{1n}} \begin{pmatrix} i \\ -(1+n\nu) \end{pmatrix} e^{i(1+n\nu)\theta} \exp(i(1+n\nu)t) + \text{c.c.} \\ & + z^2(s) \frac{(c_{11} \xi_1(0) \xi_1(-r_0) + c_{02} \xi_1^2(-r_0) + c_{20} \xi_1^2(0))}{\mathcal{N}_{20}} \\ & \times \begin{pmatrix} 1 \\ 2i \end{pmatrix} e^{2i\theta} \exp(2it) + \text{c.c.} \\ & + |z(s)|^2 \frac{(c_{11}(\xi_1(0) \bar{\xi}_1(-r_0) + \bar{\xi}_1(0) \xi_1(-r_0)) + 2c_{20} |\xi_1|^2(0) + 2c_{02} |\xi_1|^2(-r_0))}{\mathcal{N}_{00}} \begin{pmatrix} 1 \\ 0 \end{pmatrix}, \end{aligned}$$

where

$$\mathcal{N}_{mm} = B_0 - (m + n\nu)^2 + iA_0(m + n\nu) + C_0 e^{-i(m+n\nu)r_0}. \quad (26)$$

3.3. The Solution to $\mathcal{O}(\varepsilon^2)$

Employing the above results yields

$$\dot{X}_t^3(\theta; s) = \begin{cases} \frac{dX_t^3(\theta^+; s)}{d\theta}, & -r_0 \leq \theta < 0, \\ LX_t^3(\theta; s) - \begin{pmatrix} F_1^3(t; s) + \hat{F}_1^3(t; s) \\ F_2^3(t; s) + \hat{F}_2^3(t; s) \end{pmatrix}, & \theta = 0, \end{cases} \quad (27)$$

where the terms that are linear in $z(s)$ are given by

$$\begin{aligned} F_1^3(t; s) &= \xi_1(0)\dot{z}(s) \exp(it), \\ F_2^3(t; s) &= [\xi_2(0) - r_0 C_0 \xi_1(-r_0)]\dot{z}(s) \exp(it) \\ &\quad + C_0 \xi_1 \sum_{\substack{m, n \neq 0 \\ -1}}^1 \left(\frac{C_0(1 + n\nu)e^{-i(1+n\nu)r_0}}{\mathcal{N}_{1n}} - \frac{1}{2} \right) \mu_n \mu_m e^{i(m+n)\nu t} z(s) \exp(it) \\ &\quad + \alpha(A_1 \xi_2(0) + B_1 \xi_1(0) + C_1 \xi_1(-r_0))z(s) \exp(it), \end{aligned}$$

and the expression for the nonlinear terms $\hat{F}^3(t; s)$ are long and most of these terms do not contribute to the dynamics of $z(s)$ governed by the bifurcation equations. Hence $\hat{F}^3(t; s)$ is not explicitly given here. The nonhomogeneous equation at $\theta = 0$,

$$JX^3(t; s) = \begin{pmatrix} F_1^3(t; s) + \hat{F}_1^3(t; s) \\ F_2^3(t; s) + \hat{F}_2^3(t; s) \end{pmatrix}, \quad (28)$$

is solvable for $X^3(t; s) \in \mathcal{D}(J)$, if and only if (22) holds, i.e.,

$$\frac{1}{2\pi \bar{N}} \int_0^{2\pi} \begin{pmatrix} A_0 + i \\ 1 \end{pmatrix}^T \begin{pmatrix} F_1^2(t; s) \\ F_2^2(t; s) \end{pmatrix} dt = 0. \quad (29)$$

This yields the necessary differential equation in terms of the slow-time s for the unknown amplitude, $z(s)$, i.e.,

$$\boxed{\dot{z}(s) - \alpha \lambda' z(s) - |\mu|^2 S(r_0, \nu) z(s) - \Lambda(r_0), |z(s)|^2 z(s) = 0}, \quad (30)$$

where

$$\begin{aligned} \lambda' &= -\frac{1}{N}(C_1 e^{-ir_0} + iA_1 + B_1), \quad N = A_0 + 2i - r_0 C_0 \exp(-ir_0), \\ S(r_0, \nu) &= \frac{C_0 e^{-ir_0}}{N} \sum_{\substack{n \neq 0 \\ -1}}^1 \left(\frac{1}{2} - \frac{C_0(1 + n\nu)e^{-i(1+n\nu)r_0}}{B_0 - (1 + n\nu)^2 + C_0 e^{-i(1+n\nu)r_0} + i(1 + n\nu)A_0} \right), \\ \Lambda(r_0) &= \left(c_{12} + \frac{c_{11}(2c_{02} + c_{11})}{B_0 + C_0} + \frac{2c_{11}c_{02} + c_{11}c_{20} + 2c_{20}c_{02}}{2iA_0 - 4 + B_0 + C_0 e^{-2ir_0}} \right) \frac{e^{-2ir_0}}{N} \end{aligned}$$

$$\begin{aligned}
 & + \left(c_{21} + \frac{c_{11}(c_{11} + 2c_{20})}{B_0 + C_0} + \frac{c_{11}c_{20}}{2iA_0 - 4 + B_0 + C_0e^{-2ir_0}} \right) \frac{e^{ir_0}}{N} \\
 & + \left(3c_{03} + 2c_{21} + \frac{4c_{02}^2 + c_{11}^2 + 4c_{20}c_{02} + 4c_{11}c_{20} + 2c_{11}c_{02}}{B_0 + C_0} \right. \\
 & \quad \left. + \frac{2c_{20}c_{02} + 2c_{11}c_{20} + c_{11}c_{02}}{2iA_0 - 4 + B_0 + C_0e^{-2ir_0}} \right) \frac{e^{-ir_0}}{N} \\
 & \frac{3c_{30} + 2c_{12}}{N} + \frac{4c_{20}c_{02} + c_{11}^2 + 4c_{20}^2 + 2c_{11}c_{20} + 4c_{11}c_{02}}{N(B_0 + C_0)} \\
 & + \frac{2c_{02}^2e^{-3ir_0} + c_{11}^2e^{-3ir_0} + c_{11}c_{02}e^{-4ir_0} + 2c_{20}^2 + c_{11}^2}{N(2iA_0 - 4 + B_0 + C_0e^{-2ir_0})},
 \end{aligned}$$

and the coefficients in terms of machine tool parameters are defined in Appendix A. Hence, the main objective of this paper can now be answered by studying the reduced nonlinear equation (30), which represents the “normal form” of the original system (7) with periodic time delay.

4. Stability and Bifurcation Analysis

Letting $z(s) = r(s) \exp(i\phi(s))$, we can rewrite (30) in polar coordinates as

$$\begin{aligned}
 \dot{r}(s) &= [\alpha\delta'_c + \mathcal{R}(r_0, \nu)|\mu|^2 + \Lambda^{Re}(r_0)r^2(s)]r(s), \\
 \dot{\phi}(s) &= \alpha\omega' + \mathcal{I}(r_0, \nu)|\mu|^2 + \Lambda^{Im}(r_0)r^2(s),
 \end{aligned} \tag{31}$$

where δ'_c is the crossing condition, $\mathcal{R}(r_0, \nu)$ and $\mathcal{I}(r_0, \nu)$ are the real and imaginary parts of $S(r_0, \nu)$, and $\Lambda^{Re}(r_0)$ and $\Lambda^{Im}(r_0)$ are the real and imaginary parts of the nonlinear coefficient $\Lambda(r_0)$. Since there are no resonances, the bifurcation equations (31) have \mathbb{S}^1 symmetry and the phase is decoupled from the amplitude of the nonlinear response.

First, we clarify the mechanism for the suppression of regenerative chatter, by examining the stability of the trivial solution of (31), which is governed by

$$\dot{r}(s) = (\alpha\delta'_c + |\mu|^2 \mathcal{R}(r_0, \nu))r(s), \tag{32}$$

where an explicit formula for the crossing condition, δ'_c , is given in Appendix C, and the variation of δ'_c is given in Figure 4. When $\mu = 0$, it is obvious that the machine tool system is unstable for $\alpha > 0$; chatter instability for constant spindle speed is discussed in Section 2 (see Figure 2). Hence, stabilization is possible only if the real part of $S(r_0, \nu)$ is negative, i.e.,

$$\boxed{\mathcal{R}(r_0, \nu) = \sum_{\substack{n \neq 0 \\ -1}}^1 \frac{\mathcal{A}_n^c \cos(n\nu r_0) + \mathcal{A}_n^s \sin(n\nu r_0) + \mathcal{A}_n^0}{\mathcal{B}_n^c \cos(n\nu r_0) + \mathcal{B}_n^s \sin(n\nu r_0) + \mathcal{B}_n^0} < 0}, \tag{33}$$

where the coefficients \mathcal{A}_n s and \mathcal{B}_n s are given in Appendix C. It is obvious from the above expression (33) that $\mathcal{R}(r_0, \nu)$ fluctuates with ν , and it is important to determine

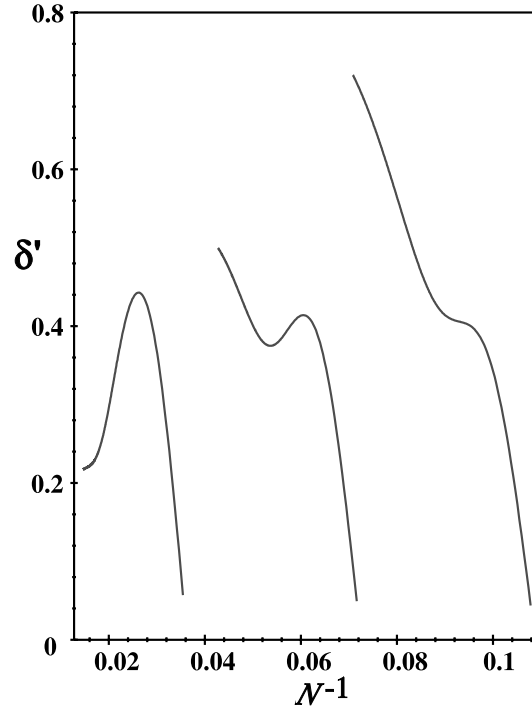


Fig. 3. Crossing condition, δ' for $p = 173.25$, and $\Delta = 0.041845$.

the optimal value of ν for which $\mathcal{R}(r_0, \nu)$ has an infimum. Since the coefficients \mathcal{A}_n s and \mathcal{B}_n s are long and contain various powers of ν , it involves some tedious computations to determine this optimal value of ν explicitly. Instead, by plotting the variation of $\mathcal{R}(r_0, \nu)$ and its derivative with ν , we identify the optimal frequency of the spindle speed variation. They are obtained in each parabolic lobe, and the variation for the second parabolic lobe at three values of τ_c is shown in Figure 4.

As expected, the stability of the system improved with increasing SSV-frequency ν , and the value of the optimal SSV-frequency varies from region to region. From (33), we derive a new stability boundary which depends on the SSV-amplitude μ and SSV-frequency ν and the bifurcation parameter α . The new stability boundary, in terms of the width of cut, is given as

$$\alpha_{cr}^{ssv} = -|\mu|^2 \frac{\mathcal{R}(r_0, \nu)}{\delta'_c}. \tag{34}$$

Hence, positive values of α_{cr}^{ssv} imply stabilization and greater widths of cut that could be achieved without chatter, while negative values of α_{cr}^{ssv} imply further destabilization. For a fixed value of amplitude $\mu = 1$ of the spindle speed modulation, we determine the new critical value of α for three different values of frequency $\nu = 0.1$, $\nu = 0.2$, and $\nu = 0.3$. The new widths of cut are plotted in Figure 4, which also shows that for the value close to $\nu = 0.3$, we obtain better widths of cut as indicated in Figure 4. Finally,

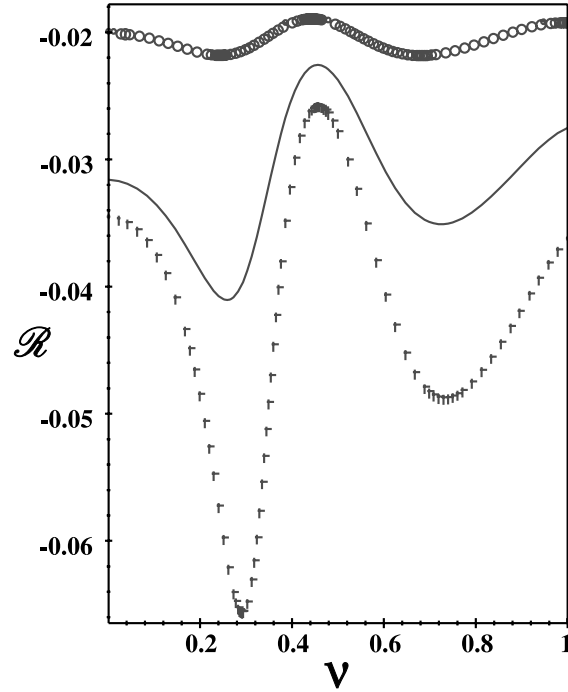


Fig. 4. Variation of Stability Index $\mathcal{R}(r_0, \nu)$ with SSV frequency ν at $\tau_c = 0.05361$ (\circ), $\tau_c = 0.04886$ ($-$), $\tau_c = 0.04552$ ($+$).

we show in Figure 4 a modest level of increase of stability, and the curves have similar parabolic lobes as the constant stability curves. The actual value of the improved width of cut can easily be calculated by multiplying the value from Figure 4 by the factor $|\mu|^2$, which denotes the square of the amplitude of the spindle speed modulation.

From (31), we have

$$r_1 = 0, \quad r_2 = \sqrt{-\frac{\alpha\delta' + \mathcal{R}(r_0, \nu)|\mu|^2}{\Lambda^{Re}(r_0)}} \quad (35)$$

as the stationary solutions. The nontrivial solution indicates a delayed Hopf bifurcation, and the sign of $\Lambda^{Re}(r_0)$ governs the qualitative behavior close to the new bifurcation point α_{cr}^{ssv} . The variation of $\Lambda^{Re}(r_0)$ is given in Figure 4. The bifurcation is supercritical when $\Lambda^{Re}(r_0) < 0$, and subcritical when $\Lambda^{Re}(r_0) > 0$. In both cases the trivial solution becomes unstable for widths of cut larger than α_{cr}^{ssv} . However in subcritical bifurcations the increase of oscillation amplitude is sudden and sometimes very dangerous—a well-known result in classical bifurcation theory.

From the numerical values of the bifurcation coefficient $\Lambda^{Re}(r_0)$ presented in Figure 4, it is clear that for the nonlinear parameter values case (i) $\beta_2 = 479.3$, $\beta_3 = 264500.0$, $\hat{\beta}_2 = 5.668$, $\hat{\beta}_3 = -3715.2$; case (ii) $\beta_2 = 0.0$, $\beta_3 = 0.0$, $\hat{\beta}_2 = 5.668$, $\hat{\beta}_3 = -3715.2$, the delayed chatter is supercritical, while for the nonlinear parameter values

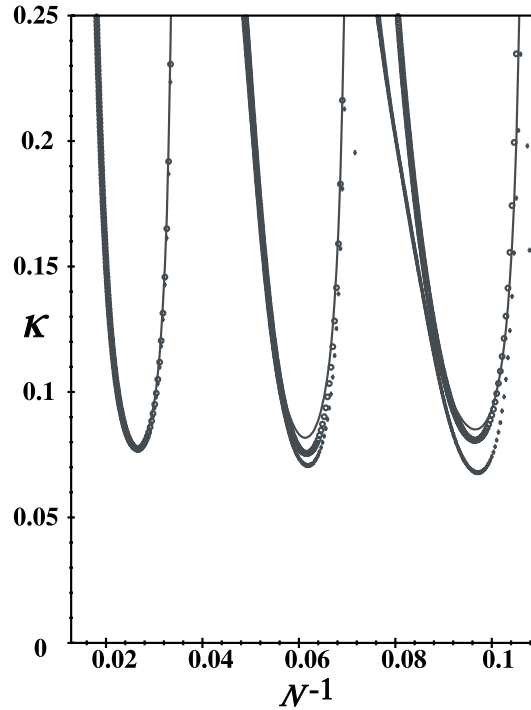


Fig. 5. Greater widths of cut for $\nu = 0.10$ (+), $\nu = 0.20$ (o), $\nu = 0.30$ (-).

case (iii) $\beta_2 = 0.0$, $\beta_3 = 0.0$, $\hat{\beta}_2 = 5.668$, $\hat{\beta}_3 = +3715.2$, the delayed chatter is subcritical. Since the nonlinear parameters β_2 and β_3 are related to the nonlinear stiffness of the machine structure, it was pointed out by Shi and Tobias [26] that these parameters have much less influence on the nonlinear dynamics than the nonlinear cutting force parameters $\hat{\beta}_2$ and $\hat{\beta}_3$. Further, if the cubic cutting force term of Kalmár-Nagy et al. [16] is compared to the $\hat{\beta}_3$ term in (1), it is found that both have the same sign for case (iii). Hence, the delayed subcritical bifurcation behavior corresponding to case (iii) agrees with the results of Kalmár-Nagy et al. [16], and correspondingly, with the experiments of Shi and Tobias [26]. Similar bifurcation behavior for the autonomous regenerative system (7) was obtained by Liang [17], for the first time, using both the Lyapunov-Schmidt and center-manifold methods.

5. Results and Conclusions

In this paper we have provided a more transparent derivation of the chatter suppression results than those available in the literature [24], [25], [18], [30], [15], which show stabilization by periodic fluctuations in delay of a second-order delay differential equation. An explicit formula (34) for the stability boundaries was obtained in terms of modulation amplitude, μ , and frequency, ν . Since these results are explicit, making use of the ex-

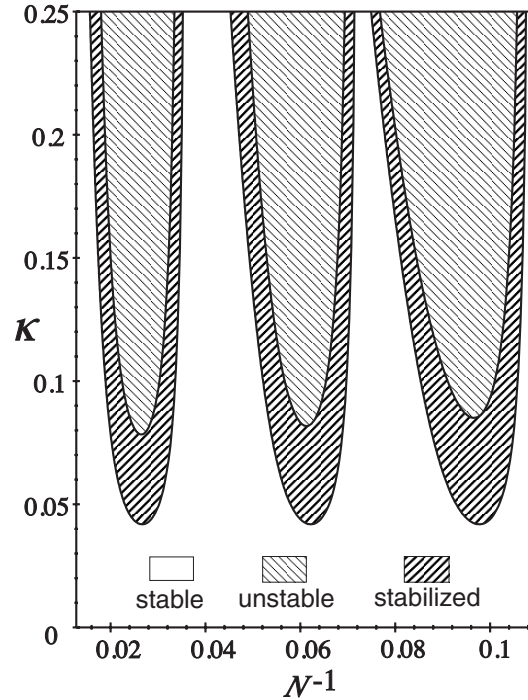


Fig. 6. Stability chart for constant speed and SSV with $\nu = 0.30$.

pression (33), we have showed how an optimal frequency ν can be determined to achieve greater widths of cut. We have also emphasized several key points that shed light on the underlying mathematical structure and the stabilization mechanism that exist in such infinite-dimensional systems with one critical mode. Finally, we predicted analytically the nonlinear behavior beyond the *new threshold of chatter* using three possible combinations of the nonlinear stiffness and cutting force coefficients. The delayed subcritical bifurcation behavior corresponding to case (iii), for the problem with only cutting force characteristics, agrees with the results of Kalmár-Nagy et al. [16].

As indicated in Section 1, experimental results and analogue computer simulations [24], [25] have confirmed that there were significant transient phenomena associated with SSV. The *transient vibrations often attained very large amplitudes* before decaying. Furthermore, the amplitude of the transient vibrations increased with increased width of cut. Hence, in the presence of SSV, the stability boundary from the linear model provides an improved chatter threshold only if the delayed bifurcation is supercritical. However, if the delayed bifurcation is subcritical, the stabilization due to SSV will not be significant due to the fact that any small disturbance can cause the oscillations to jump from small to large amplitudes. In this situation, designers can develop systematic control design techniques, based on (34) and (35), in order to suppress undesirable vibrations which can lead to poor surface finish and component failures. Such control techniques are of critical importance to operational safety as well as cost.

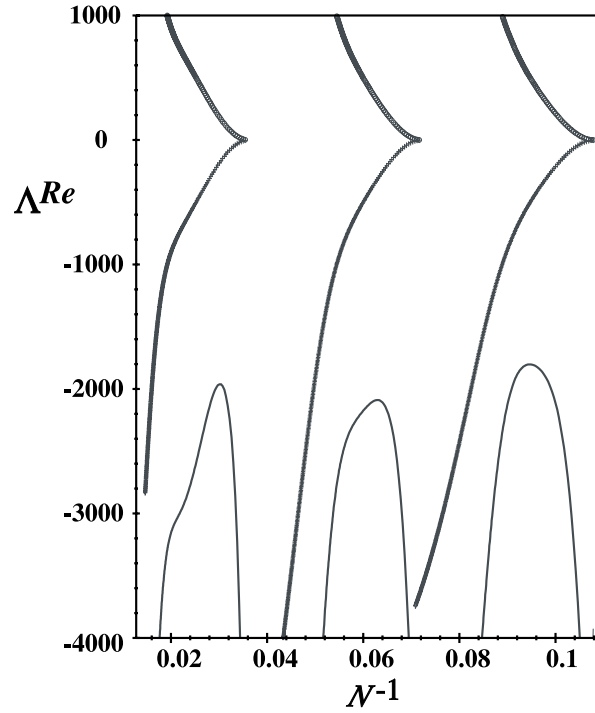


Fig. 7. Bifurcation coefficient $\Lambda^{Re}(r_0)$ for case (i) (-) $\beta_2 = 479.3, \beta_3 = 264500.0, \hat{\beta}_2 = 5.668, \hat{\beta}_3 = -3715.2$; case (ii) (+) $\beta_2 = 0.0, \beta_3 = 0.0, \hat{\beta}_2 = 5.668, \hat{\beta}_3 = -3715.2$; case (iii) (o) $\beta_2 = 0.0, \beta_3 = 0.0, \hat{\beta}_2 = 5.668, \hat{\beta}_3 = +3715.2$.

Appendix A. Coefficients of Linear and Nonlinear Terms

The linear and nonlinear terms in (8) are given explicitly as

$$A(\alpha) = A_0 + A_1\alpha, \quad B(\alpha) = B_0 + B_1\alpha, \quad C(\alpha) = C_0 + C_1\alpha.$$

In the case of fixed spindle speed, with varying *width-of-cut*, we choose κ as the bifurcation parameter while r_0 is fixed. The coefficients, in terms of machine tool parameters, are given as

$$\begin{aligned} A_0 &= 2\zeta_c\omega_p = \Delta\omega_p^2, & B_0 &= \omega_p^2(1 + \kappa_c), & C_0 &= -\kappa_c\omega_p^2, \\ A_1 &= 2\zeta'_c\omega_p = -\Delta\omega_p^2\omega'_c, & B_1 &= \omega_p^2, & C_1 &= -\omega_p^2, \\ c_{20}(0) &= -\omega_p^2(\beta_2 + \kappa_c\hat{\beta}_2), & c_{11}(0) &= 2\kappa_c\omega_p^2\hat{\beta}_2, & c_{02}(0) &= -\kappa_c\omega_p^2\hat{\beta}_2, \\ c_{30}(0) &= -\omega_p^2(\beta_3 + \kappa_c\hat{\beta}_3), & c_{03}(0) &= \kappa_c\omega_p^2\hat{\beta}_3, & -c_{12}(0) &= c_{21}(0) = 3c_{03}(0). \end{aligned}$$

The machine tool parameters are evaluated empirically through experiments and are given below:

$$\begin{cases} h = 78250 \text{ lb rad/in}, & k_0 = 1.87 \cdot 10^6 \text{ lb rad/in}, \\ p = 173.25 \text{ c/sec}, & z = 24 \text{ HSS blades}, \\ \beta_2 = 479.3 \text{ 1/in}, & \beta_3 = 264500 \text{ 1/in}^2, \\ \hat{\beta}_2 = 5.668 \text{ 1/in}, & \hat{\beta}_3 = -3715.2 \text{ 1/in}^2. \end{cases} \quad (36)$$

Appendix B. Analysis of Functional Differential Equations

Here we state some facts about the homogeneous equation

$$\dot{X}_t^1(\theta) = \mathbf{A}X_t^1(\theta),$$

where the operator \mathbf{A} is

$$\mathbf{A}\phi(\theta) = \begin{cases} \frac{d\phi(\theta^+)}{d\theta}, & -r_0 \leq \theta < 0, \\ \int_{-r_0}^0 [d\eta(\theta)]\phi(\theta), & \theta = 0, \end{cases} \quad (37)$$

and the adjoint operator of \mathbf{A} is

$$\mathbf{A}^*\psi(\tau) = \begin{cases} -\frac{d\psi(\tau)}{d\tau}, & 0 < \tau \leq r_0, \\ \int_{-r_0}^0 [d\eta(\theta)]^T \psi(-\theta), & \tau = 0. \end{cases} \quad (38)$$

Suppressing the slow-time parameter s , the eigenfunction $\xi(\theta)$, $-r_0 \leq \theta \leq 0$ corresponding to simple eigenvalue i or the basis of $\mathcal{N}(\mathbf{A} - \lambda\mathbf{I})$ for $\lambda = i$, is

$$\xi(\theta) = \xi(0)e^{i\theta} \quad \text{and} \quad \xi(0) = \begin{pmatrix} 1 \\ i \end{pmatrix}, \quad (39)$$

where $\xi(0)$ satisfies

$$i\xi(0) = \int_{-r_0}^0 \left\{ \begin{pmatrix} 0 & 1 \\ -B_0 & -A_0 \end{pmatrix} \delta(\theta) + \begin{pmatrix} 0 & 0 \\ -C_0 & 0 \end{pmatrix} \delta(\theta + r_0) \right\} \xi(0)e^{i\theta} d\theta.$$

Similarly the eigenfunction $\xi^*(\tau)$, $0 \leq \tau \leq r_0$, corresponding to simple eigenvalue $-i$ or the basis of $\mathcal{N}(\mathbf{A}^* - \bar{\lambda}\mathbf{I})$ for $\bar{\lambda} = -i$ is given by

$$\xi^*(\tau) = \xi^*(0)e^{i\tau} \quad \text{and} \quad \xi^*(0) = \frac{1}{N} \begin{pmatrix} A_0 - i \\ 1 \end{pmatrix}, \quad (40)$$

where $\xi^*(0)$ satisfies

$$-i\xi^*(0) = \int_{-r_0}^0 \left\{ \begin{pmatrix} 0 & -B_0 \\ 1 & -A_0 \end{pmatrix} \delta(\theta) + \begin{pmatrix} 0 & -C_0 \\ 0 & 0 \end{pmatrix} \delta(\theta + r_0) \right\} \xi^*(0)e^{-i\theta} d\theta.$$

The bilinear form that determines the formal adjoint operator \mathbf{A}^* simplifies to

$$\langle \xi^*(\tau), \xi(\theta) \rangle = \bar{\xi}^{*T}(0) \cdot \xi(0) - C_0 \int_{-r_0}^0 \bar{\xi}_2^*(s - \theta) \xi_1(s) ds. \quad (41)$$

The normalization condition

$$\langle \xi^*(\tau), \xi(\theta) \rangle = 1, \quad \langle \xi^*(\tau), \bar{\xi}(\theta) \rangle = 0, \quad \langle \bar{\xi}^*(\tau), \xi(\theta) \rangle = 0 \quad (42)$$

yields

$$N = A_0 + 2i - r_0 C_0 \exp(-ir_0).$$

Making use of the above definitions, it can be shown ([6], Chapter 7) that any function $\phi \in \mathcal{C}([-r_0, 0], \mathbb{R}^2)$ belongs to the range of the operator $(A - i)$ if and only if ϕ satisfies $\langle \phi, \xi^* \rangle = 0$. The consequence of this is the fact $\mathcal{C}([-r_0, 0], \mathbb{R}^2)$ has a decomposition of the form

$$\mathcal{C}([-r_0, 0], \mathbb{R}^2) = \mathcal{N}(\mathbf{A} - i\mathbf{I}) \oplus \mathcal{R}(\mathbf{A} - i\mathbf{I}),$$

where

$$\mathcal{N}(\mathbf{A} - i\mathbf{I}) \stackrel{\text{def}}{=} \{\phi: (\mathbf{A} - i\mathbf{I})\phi = 0\} \quad \text{and} \quad \mathcal{R}(\mathbf{A} - i\mathbf{I}) \stackrel{\text{def}}{=} \{\phi: \langle \phi, \xi^* \rangle = 0\}.$$

Appendix C. Coefficients of Stability Index

The transversality condition at the criticality is given by the derivative of the real part of the normalized eigenvalue, which can be found from equation (3) as

$$\begin{aligned} \delta'_c &= \frac{\chi + ((\Delta - \kappa_c r_0) \cos(r_0) - \Delta + \kappa_c r_0) \omega_p^4 - 2\omega_p^2 \sin(r_0)}{(\Delta^2 + 2\Delta r_0 \kappa_c \cos(r_0) + r_0^2 \kappa_c^2) \omega_p^4 - 4r_0 \kappa_c \omega_p^2 \sin(r_0) + 4}, \\ \chi &\stackrel{\text{def}}{=} (2 - \omega_p^2 r_0 \kappa_c \sin(r_0)) \Delta \omega_p^2 \omega'_c, \\ \omega'_c &= -\frac{\omega_p^2 (\omega_p^2 (\Delta + \kappa_c r_0) \sin(r_0) + 2 \cos(r_0) - 2)}{\Delta \omega_p^4 r_0 \kappa_c \cos(r_0) + 4 - 4r_0 \kappa_c \omega_p^2 \sin(r_0) + r_0^2 \kappa_c^2 \omega_p^4}, \end{aligned}$$

where ω'_c is the derivative of the imaginary part of the normalized eigenvalue at criticality.

The coefficients \mathcal{A}_n s and \mathcal{B}_n s of the stability index (33) are given below:

$$\begin{aligned} \mathcal{A}_n^c &= -2n\nu r_0(1 + n\nu)A_0^4 + (-4n\nu(1 + n\nu)B_0 - 2n\nu(n\nu + 2)(1 + n\nu))A_0^3 \\ &\quad + (-2n\nu r_0(n\nu + 2)B_0^2 + 2n\nu r_0(n\nu + 2)^2 B_0 - 2n\nu r_0(n\nu + 2)(1 + n\nu))A_0^2 \\ &\quad + (-2B_0^3 n\nu + 2n\nu(n\nu + 3)(1 + n\nu)B_0^2 + 2n\nu(1 + 2n\nu + 2n^2\nu^2)B_0 \\ &\quad - 6n\nu(1 + n\nu)^2 A_0 - 2r_0 B_0^4 n\nu + 2n\nu r_0(4 + 2n\nu + n^2\nu^2)B_0^3 \\ &\quad - 6n\nu r_0(2 + 2n\nu + n^2\nu^2)B_0^2 + 2n\nu r_0(6n\nu + 4 + 3n^2\nu^2)B_0 \\ &\quad - 2n\nu r_0(1 + n\nu)^2, \end{aligned}$$

$$\begin{aligned} \mathcal{A}_n^s = & -2(1 + nv)^2 A_0^4 + (2r_0 B_0 n^2 v^2 + 2v^2 r_0 n^2 (1 + nv)) A_0^3 \\ & + ((-2 + 2n^2 v^2 - 2nv) B_0^2 + 2(nv + 2)(2n^2 v^2 + 2 + 3nv) B_0 \\ & - 2(1 + nv)(4nv + 3)) A_0^2 + (2r_0 B_0^3 n^2 v^2 + 2v^2 r_0 n^2 (nv - 1) B_0^2 \\ & - 2v^2 r_0 n^2 (2nv + 1) B_0 + 2v^2 r_0 n^2 (1 + nv)) A_0 + (4 + 4nv) B_0^3 \\ & - 4(1 + nv)(n^2 v^2 + 3 + 2nv) B_0^2 + 4(1 + nv)(2n^2 v^2 + 3 + 4nv) B_0 \\ & - 4(1 + nv)^3, \end{aligned}$$

$$\begin{aligned} \mathcal{A}_n^0 = & -nv(-2B_0^2 - 2B_0nv + 6nv + nvA_0^2 + 2 + n^3v^3 + 4n^2v^2) \\ & \cdot (A_0 + r_0 + A_0^2r_0 - 2r_0B_0 + B_0A_0 + r_0B_0^2), \\ \mathcal{B}_n^c = & 4(A_0^2 + 2r_0A_0 + 2A_0r_0B_0 + r_0^2 - 2r_0^2B_0 + r_0^2B_0^2 + 4 + r_0^2A_0^2) \\ & \cdot (-B_0^2 + 2B_0 + 2B_0nv + B_0n^2v^2 - 2nv - n^2v^2 - 1 - nvA_0^2 - A_0^2), \\ \mathcal{B}_n^s = & 4v(A_0^2 + 2r_0A_0 + 2A_0r_0B_0 + r_0^2 - 2r_0^2B_0 + r_0^2B_0^2 + 4 + r_0^2A_0^2) \\ & \cdot nA_0(nv + 1 + B_0), \\ \mathcal{B}_n^0 = & 2(A_0^2 + 2r_0A_0 + 2A_0r_0B_0 + r_0^2 - 2r_0^2B_0 + r_0^2B_0^2 + 4 + r_0^2A_0^2) \\ & \cdot (2B_0^2 - 2B_0n^2v^2 - 4B_0 - 4B_0nv + 2A_0^2 + 2 + n^4v^4 + 2nvA_0^2 \\ & + 4nv + n^2v^2A_0^2 + 6n^2v^2 + 4n^3v^3). \end{aligned}$$

Acknowledgments

The authors would like to acknowledge the support of the Office of Naval Research under grant number N001-15-005, and of the National Science Foundation under grant number CMS 00-84944. The first author would also like to thank Professors Mustapha S. Fofana, Francis C. Moon, and Gábor Stépán for introducing the exciting field of machine tool chatter. The author's initial curiosity in the industrial use of spindle speed variation for chatter suppression was also confirmed by Professor Gábor Stépán during his visit to the University of Illinois at Urbana-Champaign in September 2000. Reference [23] was added after our paper was accepted for publication; the authors would like to thank Professor A. G. Ulsoy for bringing this reference to their attention.

References

- [1] Balachandran, B. Nonlinear Dynamics of Milling Processes. *Philosophical Transactions of the Royal Society*, 359 (2001), 793–819.
- [2] Bancroft, S., Hale, J. K., and Sweet, D. Alternative Problems for Nonlinear Functional Equations. *Journal of Differential Equations*, 4 (1968), 40–56.
- [3] Carr, J. *Applications of Center Manifold Theory*. Springer-Verlag, New York (1981).
- [4] Chafee, N. A Bifurcation Problem for a Functional Differential Equation of Finitely Retarded Type. *Journal of Mathematical Analysis and Applications*, 35 (1971), 312–348.

- [5] Demir, A., and Namachchivaya, N. Sri, and Langford, W. F. *Nonlinear Delay Equations with Fluctuating Delay: Application to Regenerative Chatter*, ASME, New York, 2002, 12 pp., CD-ROM.
- [6] Hale, J. K. *Theory of Functional Differential Equations*. Springer-Verlag, New York (1977).
- [7] Hale, J. K. Nonlinear Oscillations in Equations with Delays. *Nonlinear Oscillations in Biology*. Edited by Frank C. Hoppensteadt, pp. 157–185. American Mathematical Society, Providence, RI (1979).
- [8] Hanna, N. A., and Tobias, S. A. A Theory of Nonlinear Regenerative Chatter. *Journal of Engineering for Industry*, Transactions of the ASME 35 (1974), 247–255.
- [9] Hassard, B. D., Kazarinoff, N. D., and Wan, Y.-H. *Theory and Applications of Hopf Bifurcation*. London Mathematical Society Lecture Note Series, 41. Cambridge University Press, Cambridge (1983).
- [10] an der Heiden, U. Delays in Physiological Systems. *Journal of Mathematical Biology*, 8 (1979), 345–364.
- [11] Hosi, T., and Sato, M. Study of Practical Application of Fluctuating Speed Cutting for Regenerative Chatter Control. *Annals of the CIRP*, 25 (1977), 175–179.
- [12] Inamura, T., and Sata, T. Stability Analysis of Cutting under Varying Spindle Speed. *Annals of the CIRP*, 23 (1974), 119–120.
- [13] Inamura, T., and Sata, T. Stability Analysis of Cutting under Varying Spindle Speed. *Journal of the Faculty of Engineering*, University of Tokyo-B, 23(1) (1975), 13–29.
- [14] Insuperger, T., Stépán, G., and Namachchivaya, N. Sri. Comparison of the Dynamics of Low Immersion Milling and Cutting with Varying Spindle Speed. *18th Biennial Conference on Mechanical Vibration and Noise*, DETC2001/VIB-21616, ASME Design Engineering Technical Conferences, Pittsburgh, Pennsylvania, September 9–12, 2001.
- [15] Jayaram, S., Kapoor, S. G., and DeVor, R. E. Analytical Stability Analysis of Variable Speed Machining. *Journal of Manufacturing Science and Engineering*, Transactions of the ASME 122 (2000), 391–397.
- [16] Kalmár-Nagy, T., Stépán, G., and Moon, F. C. Subcritical Hopf bifurcation in the delay equation model for machine tool vibrations. *Nonlinear Dynamics*, 26 (2001), 121–142.
- [17] Liang, Yan. *Nonlinear Dynamics in Manufacturing Process*. Master's Thesis, University of Illinois (2000).
- [18] Lin, S. C., Kapoor, S. G., and DeVor, R. E. The Effects of Variable Speed Cutting on Vibration Control in Face Milling. *Journal of Engineering for Industry*, Transactions of the ASME 112 (1990), 1–11.
- [19] MacDonald, N. *Biological Delay Systems: Linear Stability Theory*. Cambridge University Press, Cambridge (1989).
- [20] Moon, F. C. *Dynamics and Chaos in Manufacturing Process*. John Wiley & Sons, Inc., New York (1998).
- [21] Namachchivaya, N. Sri, and Van Roessel, H. J. *A Center Manifold Analysis of Variable Speed Machining*. Submitted for publication (2002).
- [22] Nayfeh, A. H., Chin, C. M., and Pratt, J. Perturbation Methods in Nonlinear Dynamics: Applications to Machining Dynamics. *Journal of Manufacturing Science and Engineering*, Transactions of the ASME 119 (1974), 485–493.
- [23] Pakdemirli, M., and Ulsoy, A. G. Perturbation Analysis of Spindle Speed Variation in Machine Tool Chatter. *Journal of Vibration and Control*, 3 (1997), 261–278.
- [24] Sexton, J. S., Miline, R. D., and Stone, B. J. The Stability of Machining with Continuously Varying Spindle Speed. *Applied Mathematics and Modelling*, 1 (1977), 311–318.
- [25] Sexton, J. S., and Stone, B. J. The Stability of Machining with Continuously Varying Spindle Speed. *Annals of the CIRP*, 27 (1978), 321–326.

- [26] Shi, H. M., and Tobias, S. A. Theory of finite amplitude machine tool instability. *International Journal of Machine Tool Design and Research*, 24(1) (1984), 45–69.
- [27] Stépán, G. *Retarded Dynamical Systems: Stability and Characteristic Functions*. Longman, Harlow, UK (1989).
- [28] Takemura, T., Kitamura, T., Hoshi, T., and Okushima, K. Active Suppression of Chatter by Programmed Variation of Spindle Speed. *Annals of the CIRP*, 23 (1974), 121–122.
- [29] Tsao, T. C., McCarthy, M. W., and Kapoor, S. G. A New Approach to Stability Analysis of Variable Speed Machining Systems. *International Journal of Machine Tools Manufacture*, 33 (1993), 791–808.
- [30] Zhang, H., Ni, J., and Shi, H. Machining Chatter Suppression by Means of Spindle Speed Variation, Part I: The Numerical Simulation. *S. M. Wu Symposium*, 1 (1994), 161–167.